Energetic processes in macroscopic fractal structures

B. M. Smirnov

Institute of High Temperatures, Academy of Sciences of the USSR, Moscow
(Submitted December 7, 1990)
Usp. Fiz. Nauk **161**, 171–200 (June 1991)

Macroscopic fractal systems, aerogel and fractal fiber, have a high specific surface energy. Mechanisms of the process of structure densification which leads to the transformation of the surface energy into thermal energy are considered. Transport processes inside macroscopic fractal systems are investigated. Conditions of the thermal explosion and the character of propagation of the thermal wave inside these systems are analyzed.

1. INTRODUCTION

Aerogels which are formed from small particles in solutions, and fractal fibers, which are formed from a non-equilibrium low-temperature plasma in an external electric field, are macroscopic fractal structures. Fractal clusters (fractal aggregates) are the small elements of these structures. The fractal property of these objects is essentially that, if one passes a sphere of a definite radius through one of the cluster particles and then changes this radius then, in a definite range of radius values, on an average, the density of the material inside the sphere will decrease with increasing radius.

However, this property of fractal structures is unimportant for the purpose of this paper. For us it is important that the objects under consideration are very low density structures consisting of small particles. Thus, the average density of the structural material to which we shall direct our attention in the estimates is of the order of 0.01 g/cm^3. This is a typical value for fractal fibers and is an attainable value for aerogels (aerogel specimens are created with 0.005 g/cm^3 density). In such a system, most of the volume inside the object is occupied by empty spaces. Therefore, certain processes which go on inside these structures will be analogous to processes in gases, but here their own distinguishing features will develop. For example, if we light small pieces of a match in air, it will burn for seconds, and moreover, the energy that is released here will be mostly carried away into the air due to convection. The convection of air also provides a flow of oxygen into the combustion zone. If one places the small pieces of a match in a low density aerogel that is located in air and ignites them, then there will be no convection, the arrival of oxygen in the combustion zone will be provided due to oxygen diffusion, and energy removal will be due to radiation from the flame and partly due to the thermal conductivity of air. As a result of this, combustion of the same specimen will go on not for seconds, but for minutes, and the chemical energy of the specimen will be mostly converted into radiative energy.

A large specific internal surface area is another property of the systems under consideration. The nature of the formation of such structures leads to their consisting of small particles such that an appreciable fraction of the molecules of these particles is located on their surfaces. At the same time, the chemical composition of the material (as a rule, this consists of oxides) provides a high chemical interaction energy in the systems (as in ceramics). Therefore, aerogels and fractal fibers have large specific energy supplies that are comparable with the corresponding characteristics of gunpowder and explosives. An explosion of these structures is possible. As a result of this process, an increase of the structure's density occurs, i.e., the average size of the structure's particles increases, and the system's specific surface energy decreases. The energy that is released goes to heat the system and accelerate the process. A thermal wave arises in the system which, in propagating, leads to conversion of the internal energy and to destruction of the structure.

Along with the thermal processes within fractal structures, the conditions for the thermal explosion of structures and the parameters of the thermal wave which arises here are analyzed in this paper.

2. FRACTAL GROWTH STRUCTURES

2.1. The fractal cluster

A fractal cluster (or fractal aggregate) is a system of connected solid particles. It possesses the following property. Its correlation function is

$$C(r) = \frac{\langle \rho(\mathbf{r}')\rho(\mathbf{r}'-\mathbf{r})\rangle}{\langle \rho(\mathbf{r}')\rangle}; \tag{2.1}$$

here $\rho(r)$ is the particle density at a given point, and $\langle\ \rangle$ denotes averaging over the particle positions. This equation means that if one constructs a sphere of radius r with its center located at one of the particles, counts the number of particles on the sphere, and performs this operation many times while changing the particles at the center of the sphere, then the mean density of particles on the sphere varies according to the law $r^{-\alpha}$ with change of the sphere's radius r. It follows from this that the mean density of particles inside the sphere varies according to the law:

$$\rho \sim r^{D-d}, \tag{2.2}$$

 0038-5670/91/060526-16$01.00

where $\alpha = d - D$, d is the dimensionality of space, and D is the cluster's fractal dimension. Below, we shall consider the fractal cluster as a physical object in real space, i.e., $d = 3$.

A large number of reviews and monographs have been devoted to investigating the properties of fractal clusters, the processes of their growth, and to models describing these processes.[1-15] Since a fractal cluster is of interest to us as a real physical object, let us next briefly pause for just the experimental methods for obtaining fractal clusters and the properties of such systems.

A fractal cluster is formed by the adhesion of solid particles. Processes for forming small solid particles in a gas and fluid go on in various ways. In a gas, these particles are the result of condensation of vapor formed, as a rule, by the vaporization of a solid surface by an external effect on it. Thus, in the first experiment by Forrest and Witten,[16] this effect consisted of passing a strong electric current through a wire onto which specified substances had been coated. The vaporized material cooled in the process of expanding into space, which also led to condensation and then to the aggregation into clusters of the solid particles which were being formed. The average particle radius in the structure was 3 nm to 4 nm, and a typical cluster size was several microns. This paper was the first experimental investigation of fractal clusters and laid the methodological foundations for analyzing such experiments. Fractal clusters were collected on a net and were photographed by an electron microscope. An ordinary photograph of a cluster covered an area of several square microns and included in it a part of a cluster in which a large number of particles was located. After dividing this photograph into cells by means of a grid, from the degree of filling of the corresponding cell, the authors considered it as either empty or completely filled. Such information about a photograph (in the form of zeroes or ones) was put into a computer and was processed there in this form. A cluster's fractal dimension was determined on the basis of the distance dependence for the correlation function (2.1), the fractal dimension D_α, or from the number of occupied cells as a function of the area of the photograph section picked out, the fractal dimension D_β. The results are shown in Table I. The value of the cluster's fractal dimension averaged from these data is 1.6 ± 0.07.

This method of obtaining clusters was modified in a series of papers,[17-22] where fractal clusters were finally set down onto a surface and their high efficiency in absorbing thermal radiation was used. Let us analyze one of the papers of this series,[22] where the formation of cobalt clusters was studied. Small particles of cobalt were formed in an argon atmosphere by vaporizing the metal with a traditional method[17] of using a heated tungsten spiral with conditions of convective vapor transfer. The argon pressure ranged from 0.25 torr to 10 torr. The metal particles, like soot, were collected on a copper net covered with carbon and were investigated by means of an electron microscope. The average thickness of the metallic precipitate was 10 μm to 200 μm, and moreover, the volume occupied by the cobalt particles in this layer was estimated at 10^{-4} to 0.01 of the total, i.e., the precipitate had a porous structure and pores occupied most of its volume. The average particle radius in these formations increased with increasing argon pressure, the fractal dimensions of the aggregates formed were from 1.75 to 1.9 at argon pressures from 0.9 torr to 8 torr, and the average particle radius was less than 8 nm. At argon pressures over 8 torr, the particle radius in an aggregate was more than 8 nm, and the fractal dimensions of an aggregate were from 1.9 to 2.05.

Let us notice that the fractal dimensions of clusters formed during the vaporization of a metal in an inert gas are somewhat higher than in the case of its vaporization in a vacuum. According to the measurements in Refs. 18, 19, and 20, the fractal dimensions of clusters of aluminum, nickel, and cobalt obtained during the vaporization of these metals in an argon atmosphere were from 1.75 to 1.85. Vaporization of a metal in an inert gas delays the formation process in comparison with the case of its vaporization in a vacuum, and therefore it leads to the creation of denser formations.

Another method for obtaining fractal clusters uses irradiation of different metals with laser radiation.[23,24] Then a slightly ionized metal vapor which is at high pressure (several thousand degrees temperature and several tens of atmospheres pressure) is formed near the surface. This vapor, expanding in space, cools and condenses on ions. When the temperature of the particles which are being formed is lower than the material's melting temperature, particles of the metal join into fractal clusters. Experiments have been conducted for different metals, Al, Ti, Fe, Ag, and Pt, and in a number of buffer gases (air, argon, and helium) at pressures of 4 torr and 1 atm. The qualitative nature of the results is just the same here.

These experiments have been conducted with neodymium and ruby lasers, which provide average specific radiation powers from 10^6 W/cm^2 to 10^7 W/cm^2 for ~ 0.001 sec. The irradiated surface was of the order of 1 mm^2. Different methods for acting on a surface are possible in this and similar specific energy ranges. Laser breakdown, leading to the laser energy being absorbed by the plasma and used up in ionizing it, is possible at a sufficiently high density of the vaporized plasma. Finally this leads to the occurrence of a laser flash. It is clear that the specific laser radiation power must be lower than the laser breakdown threshold in the regime under consideration. Another regime is connected with the formation of a liquid phase on the surface and the splashing of drops of liquid as a result of thermal instability. Thereby, the nature of the interaction of laser radiation with a surface can lead to different thermal regimes on the surface.[25,26] For the formation of fractal clusters, it is necessary that vaporization of the surface material occurs.

The laser method leads to the formation of a high pressure vapor, which finally creates large particles in the struc-

TABLE I. The fractal dimensions of clusters which are formed after vaporization of material.[16]

Material	Fe	Fe	Zn	Zn	SiO_2
D_α	1,69 ± 0,02	1,68 ± 0,01	1,67 ± 0,02	1,68 ± 0,02	1,55 ± 0,02
D_β	1,52 ± 0,04	1,56 ± 0,02	1,50 ± 0,04	1,60 ± 0,04	1,55 ± 0,06

ture. Their radii are usually more than 10 nm, and the size of the cluster depends on the specific power. Thus, in the case of titanium, the average size of a cluster varied from 5 μm to 25 μm as the specific laser radiation power varied from 10^6 W/cm^2 to $5 \cdot 10^6$ W/cm^2. The average particle radius was 12 nm in this case. The fractal dimension of the clusters obtained by the laser method was 1.82 ± 0.05.

One more method for obtaining clusters in a gaseous phase is associated with the burning of silicon tetrachloride in an oxygen or hydrogen-oxygen flame.[27] A powder consisting of weakly bound clusters is formed as a result of this process. Such a powder has the name of silicon soot or silicon smoke. Its specific gravity lies in the range from 0.008 g/cm^3 to 0.45 g/cm^3. Detailed investigations of such formations show[27] that their properties depend on the regime of their formation. It has been found in the indicated paper that the fractal dimensions of the clusters obtained are from 1.8 to 2.0, and a typical cluster contains 1,000 individual particles whose radii equal from 8 nm to 10 nm. This radius depends slightly on the regime of burning. However, the specific surface of a cluster that is determined from the system's adsorption properties depends on the regime of burning. Here the ratio of the maximum specific surface of clusters to the surface for the particles composing them lies in the range from 1.81 to 3.05, and depends on the regime of burning. Based on this, the authors arrive at the conclusion that the surfaces of the particles which compose the clusters are not smooth. Here the surface fractal dimension of the clusters in these experiments is between 2.0 and 2.5, and depends on the regime of burning. The methods for obtaining fractal clusters in a liquid phase are based on methods for separating one of the components of the solution in the form of particles of an extremely definite size.[28] One can regulate this size by changing the acidity of the solution while separating a definite component. The particle size is determined by the particle charge in the system. This charge at a definite particle size hinders the approach of ions of a given material to a particle, and thereby restricts the further growth of particles. Afterwards, as the material of this component is contained in particles, one can, by means of changing the acidity of the solution, remove or reduce the charge on the particles. This will lead to the formation of a fractal cluster.

The formation of fractal clusters in solutions is methodologically simpler than in gases. Nevertheless, most research is associated with the formation of fractal clusters of gold and silicon dioxide. The fractal dimension of a cluster depends on the rate of its formation, which determines the mechanism of the process. For clusters of approximately 10 nm diameter, a formation time shorter than minutes corresponds to the cluster-cluster aggregation mechanism,[30,31] when small clusters are formed from the particles in the first stage; these are then joined into clusters of larger dimensions. If this time amounts to hours and longer, then cluster growth corresponds to a reaction-limited cluster aggregation mechanism.[32-34] In this case, the probability of joining particles during their contact is low. It is easy to regulate this probability in a solution by changing the acidity and chemical composition of the solution. The fractal dimension of 1.77 ± 0.03 corresponds to the cluster-cluster aggregation mechanism, and the fractal dimension of 2.02 ± 0.06 corresponds to the reaction-limited cluster aggregation mechanism.[32-34] Some results of investigating the formation of fractal clusters in solutions are shown in Table II.

The density of a fractal cluster decreases as its size increases. Thus, the silicon dioxide clusters that are included in Table II, which have a 1 μm size and consist of particles of 4 nm radius, contain an average of 7,000 particles and have mean densities about 0.001 g/cm^3 (the fractal dimension is taken as equal to 1.6). Therefore the strength of a cluster decreases as its size increases. Estimates show[51] that a maximum size cluster contains of the order of 10^4 single particles, and its density is approximately four orders of magnitude less than the density of the material of its particles.

2.2. Aerogel

An aerogel is a macroscopic system consisting of fractal clusters. The properties of an aerogel and the methods for

TABLE II. The formation of fractal clusters in solutions.

Cluster material	Particle radius, nm	Fractal dimension	Reference
Gold	7,2	1,7 ± 0,1 1,77 ± 0,1	[35]
Silicon dioxide	5	—	[36]
Gold	7,5	1,8	[37]
Silicon dioxide	2,7	2,12 ± 0,05	[38]
» »	—	2,0 ± 0,1	[39]
Gold	7,5	1,77 ± 0,05 2,05 ± 0,05	[40] [40]
Silicon dioxide	11	1,75 ± 0,05 2,08 ± 0,05	[41] [41]
Gold	7,5	1,75 2,2	[42] [42]
Silicon dioxide	7	2,05 ± 0,06	[43]
» »	12	2,1 ± 0,1	[44]
» »	3,5	2,10 ± 0,03	[45]
Gold	7,5	1,8	[46]
Silicon dioxide	120	1,75 ± 0,03	[47, 48]
Gold	8	1,8 ± 0,1 2,5 ± 0,1	[49] [49]
Silicon dioxide	13,5	1,84 ± 0,08	[50]

FIG. 1. Model of a small element of aerogel.[55]

obtaining and using it are described in Refs. 14, 52, 53 and 54. The aerogel structure of a small aerogel element[55] is shown in Fig. 1. Aerogel is formed in solutions from fractal clusters, and one of the main problems here is to get rid of the solution molecules which get into the small aerogel pores along with aerogel particles. The American scientist Kistler[56–58] was able to solve this problem by carrying out the process of its formation at supercritical conditions. Following this idea, all methods for obtaining aerogel use an autoclave for this purpose and carry out the process at high temperatures and pressure. For this reason, the technology of aerogel production turns out to be complicated, and the product itself is relatively expensive, which limits the use of this specific material in various applied problems.

A large specific inner surface area is one of the features of aerogels. For specimens of silicon dioxide aerogel, this quantity lies in the range $S = 500\ \text{m}^2/\text{g}$ to $1{,}500\ \text{m}^2/\text{g}$. If one assumes that an aerogel consists of small spherical particles that are tangent to each other, then the radii r_0 of these small particles are related to the specific inner surface area of the material by the relation

$$r_0 = 3/\rho_0 S, \tag{2.3}$$

where ρ_0 is the density of the material. The parameters of some silicon dioxide aerogel specimens that have been investigated in Ref. 59 are presented in Table III. As is evident, the structure particle radius calculated from Eq. (2.3) turns out to be smaller than that found from an analysis of photographs. Evidently, just as in the case of fractal clusters,[28] the particles have an inner structure which increases their inner surface. Notwithstanding this, from now on we shall for simplicity adhere to an aerogel model, according to which its structure consists of small spheres with the same radius.

A small piece of aerogel is a fractal cluster. This is determined by the mechanism of forming an aerogel, whose growth is controlled by the adhesion of individual particles moving in the solution. Particles of aerogel material are formed in the solution in the first stage of the process, which then are joined into clusters whose sizes increase until they occupy the entire volume. In connection with this, the aerogel possesses fractal properties in a region with the dimensions

$$r_0 \ll r \ll \xi, \tag{2.4}$$

where r_0 is the size of the particles which compose it, and ξ is the correlation radius or the maximum pore size (or just the characteristic size of clusters in the process of their growth in a volume when they occupy the entire volume). For $r \ll \xi$, the aerogel is homogeneous as a whole.

In accordance with one of the properties of a fractal cluster, the mean mass density of the material $\rho(r)$ in a sphere of radius r equals

$$\rho(r) = \rho_0 (r_0/r)^{3-D}, \tag{2.5}$$

where ρ_0 is the density of the cluster material, r_0 is the average particle radius, and D is the cluster fractal dimension. It follows from this that the correlation radius ξ may be estimated from the equation

$$\xi \approx r_0 (\rho_0/\bar{\rho})^{1/(3-D)}, \tag{2.6}$$

where $\bar{\rho}$ is the mean density of the aerogel.

The cluster fractal dimension D also characterizes the pore size distribution function. Actually, let the aerogel occupy some volume V_0, i.e., it has the mass $\bar{\rho} V_0$. Let us pick out a volume which is located at a distance $r \ll \xi$ from the cluster points. The mean density of the aerogel material in this volume is given by Eq. (2.5), and since the entire mass of aerogel is concentrated in this volume, the value of this volume is

$$V(r) \sim \bar{\rho} V_0/\rho(r) \sim V_0 (r/\xi)^{3-D}.$$

Obviously all pores whose sizes are smaller than or equal to r will be included in this volume. From this, we have for the pore size distribution function

$$df \sim r^{2-D} dr, \quad r_0 \ll r \ll \xi. \tag{2.7}$$

Correspondingly, the pore volume distribution has the form[52]

$$df \sim dV/V^{D/3}, \tag{2.8}$$

where df is the relative number of pores possessing volumes in the interval from V to $V + dV$. This relation is valid for pores whose sizes are smaller than the correlation radius ξ.

TABLE III. Parameters of specimens of silicon dioxide aerogel.[59]

Density, g/cm³	Specific inner surface density, m²/g	Radii of structure particles, nm	
		From TEM*) photographs	Calculation according to Eq. (2.3)
1) 0,03	1590	4	0,9
2) 0,05	1080	5	1,3
3) 0,15	520	10	2,7
4) 0,16	740	4	1,8

*) TEM is transmission electron microscopy.

Thus, the distribution of pore sizes gives information about the fractal dimension of aerogel elements. One can obtain this distribution by studying the absorption by an aerogel of different sorbents while changing the pressure of the adsorbed components. Thus, the pore size distribution for a silicon dioxide aerogel was obtained by such a method in Ref. 60 for five aerogel specimens. Processing of the information obtained using Eq. (2.8) gives $D = 2.3 \pm 0.1$ for the fractal dimension.

The fractal dimension of an aerogel can be found, just as in the case of fractal clusters, from the scattering of fast neutrons or electrons, and also of x-radiation at small angles. If the wave vector of a particle or photon equals q, then pores of size $(q\theta)^{-1}$ are responsible for scattering at the small angle θ. The dependence on the scattering angle of the differential cross section for scattering at small angles is expressed by the fractal dimension for a cluster of size $(q\theta)^{-1}$ if the aerogel is transparent, or by the fractal dimension of the surface. Suitable measurements for a silicon dioxide aerogel were conducted in a number of papers.[61-65] Not all the results are in agreement, but in most cases the fractal dimension of the aerogel is from 2.3 to 2.4.

One more approach to investigating an aerogel using inelastic neutron scattering was formed recently. This method has been mastered well in solid state physics, enabling one to study solid state excitations and mainly the phonon spectrum. The phonon spectrum of vibrations in an aerogel corresponds to wavelengths which are considerably longer than the pore sizes, i.e., $q \ll 1/\xi$ (q is the wave vector of the vibrations, and ξ is the correlation radius). Vibrations in the range

$$1/\xi \ll q \ll 1/r_0 \qquad (2.9)$$

are called fractons and are determined by the aerogel structure in the range of sizes where its fractal properties develop. Let us represent a density dependence consisting of a fracton frequency ω in the form $g(\omega) \sim \omega^d$. The value of the exponent d will carry information about the aerogel structure in the range of sizes that correspond to the fractal properties of the aerogel. The measurements that have been conducted[62-70] give values of this exponent in the $1.3 < d < 1.8$ range for silicon dioxide aerogel. Apparently, this contradiction is resolved in Ref. 65, where two types of fractons are detected: low-frequency shear vibrations to which the exponent $d = 1.3$ corresponds, and high-frequency compressional and tensile vibrations to which $d = 1.8$ corresponds.

Let us note that investigating the fracton spectrum enables one simultaneously to find its limit, i.e., to reconstruct the correlation size ξ_{ac} of the aerogel. One can also do the very same thing from a study of the small angle scattering of neutrons or photons, which gives the correlation size ξ. According to the investigations that have been conducted, the correlation size ξ_{ac} is several times larger than ξ. For example, complicated measurements were conducted in Ref. 64 for a silicon dioxide aerogel with $\bar{\rho} = 0.245$ g/cm^3 density. They gave the aerogel fractal dimension $D = 2.33 \pm 0.05$ and the correlation size values $\xi = 14$ nm and $\xi_{ac} = 52$ nm. Let us note that Eq. (2.6) gives $\xi = 40 \pm 10$ nm for the aerogel parameters considered.

A physical substance similar in its properties to an aerogel is formed in the burning of silicon tetrachloride ($SiCl_4$) in a flame of oxygen and hydrogen. This process leads to the formation of silicon dioxide particles which join into fractal clusters. Compression of the material obtained gives laboratory specimens of millimeter and centimeter sizes with densities from 0.006 g/cm^3 to 0.500 g/cm^3. Just as in the case of aerogel, small elements of these specimens possess fractal properties. Such specimens were investigated in Ref. 71. The fractal properties of certain specimens are shown in Table IV.[71]

2.3. Fractal fibers

Fractal fibers are a new physical substance which was obtained recently[72] during laser irradiation of a metal surface (see Fig. 2). Possibly this substance has been formed repeatedly in different experiments. For example, upon the explosion of a metal wire in a vacuum as a result of the passage of an electric current through it, cobweb-like, long-lasting (of the order of a day) structures were obtained in Ref. 73; these were attached to the walls of the vacuum chamber. The authors called them filamentary aerosols and estimated their diameters, which turned out to be of the order of 10 nm. However, this preliminary information does not allow us to establish an unambiguous connection between the substance observed in Ref. 73 and fractal fiber.

Reference 72 was a continuation of the work of the authors on obtaining fractal clusters by means of laser irradiation of metal surfaces. Cobweblike structures were observed at times in these experiments. The authors investigated these structures and found the conditions when they are reliably formed; with the use of an external electric field with an intensity of several hundred volts per centimeter. Then, in a chamber with a distance between electrodes of the order of several centimeters and electrode diameters of the order of a centimeter, several tens of fibers are formed simultaneously in the space between the electrodes and are attached to them.

TABLE IV. The fractal properties of specimens obtained by compression of products of burning silicon tetrachloride in an atmosphere of oxygen and hydrogen.[71]

Density, g/liter	Fractal dimension	r_0, nm	ξ, nm
1) 130	2,60 ± 0,03	1,9 ± 0,1	13,2 ± 0,6
2) 170	2,65 ± 0,03	1,9 ± 0,1	12,1 ± 0,4
3) 340	2,64 ± 0,03	1,9 ± 0,1	10,4 ± 0,3
4) 450	2,55 ± 0,04	1,8 ± 0,1	10,0 ± 0,4
5) 8	2,41 ± 0,02	2,3 ± 0,1	31 ± 2
6) 6	2,27 ± 0,04	2,4 ± 0,1	56 ± 10
7) 10	2,29 ± 0,03	2,2 ± 0,1	52 ± 9
8) 8	2,38 ± 0,02	2,3 ± 0,1	42 ± 4

FIG. 2. A fractal fiber element.[72] On the left, a photograph in the beam of light for an ordinary microscope. On the right, an electron microscope photograph.

The times for the separate stages of the process of forming fractal fibers during laser irradiation of a surface are shown in Table V.[60,61] The first states will lead to the formation of fractal clusters. The last stage, which corresponds to the joining of clusters into structures, has fundamental significance. This stage does not occur in the absence of an electric field for two reasons. First, as the sizes of clusters increase, the process of their joining slows down sharply. Second, upon reaching a definite size, a cluster cannot grow bigger because of its limited strength. Therefore, mechanisms capable of densifying the structure as it grows must exist to create a macroscopic structure.

An electric field enables one to overcome these problems. First, an electric field aligns the dipoles on the clusters so that the interaction of these dipoles determines the approach and joining of the clusters. Second, the electric field leads to densification of the structure, which occurs in accordance with the restructuring model.[76,77] According to this model, the weak bonds which arise during the joining of clusters will be torn apart in time, and then new bonds are formed. Such a process goes on as long as the bonds do not become strong.

Fractal clusters are the composite elements of both aerogel and also fractal fiber. However, aerogels are formed at isotropic conditions in solutions, and therefore are isotropic systems. Fractal fibers are formed in an external field, and therefore are anisotropic systems; they are elongated along the field.

TABLE V. The orders of magnitude of the times of the individual stages of the process of forming fractal fibers during laser irradiation of a metal surface.[74,75]

Stage	Time, sec
1. Formation of gasdynamic bunching	10^{-8}
2. Start of condensation	10^{-5}
3. Formation of solid particles	10^{-4}
4. Formation of fractal clusters	0,1
5. Formation of a fractal fiber	10^{3}

3. TRANSFER PROCESSES IN MACROSCOPIC FRACTAL STRUCTURES

3.1. Kinetic transfer coefficients inside fractal structures

Pores in which gas is found occupy most of the volume of the structures under consideration. Processes of transferring mass, momentum, and energy in such systems can occur through this gas. Next, to determine the transfer coefficients, we shall use an approximation, according to which the mean free path of a molecule is independent of its velocity. This approximation reproduces well the nature of collisions in gases that satisfy a model of hard spheres, and thereby it describes well the nature of collisions of molecules with the particles of the structure. Using the Chapman–Enscog approximation,[78,79] we have the following expressions for the coefficients of diffusion $\mathscr{D}$, viscosity η, and of thermal conductivity $\varkappa$ in a gas:

$$\mathscr{D}=\frac{3(\pi T)^{1/2}\lambda}{8(2\mu)^{1/2}},\quad \eta=\frac{5(2\pi T\mu)^{1/2}N\lambda}{16},\quad \varkappa=\frac{75(\pi T)^{1/2}N\lambda}{64(2\mu)^{1/2}}; \tag{3.1}$$

here T is the gas temperature, N is the gas molecule density, μ is the reduced mass for the colliding molecules, and λ is the mean free path of the molecules in the gas.

These expressions refer to a one-component gas, where the mean free path of the molecules equals

$$\lambda = 1/N\sigma, \tag{3.2}$$

where σ is the diffusion collision cross section of the molecules, which is independent of the relative velocities of the

TABLE VI. Values of the coefficient of thermal conductivity of silicon dioxide aerogel at room temperature.

$\varkappa$, 10^{-5} W/cm·K	ρ, g/cm^3	Reference
4	0,105	[80, 81]
11	0,27	[80, 81]
8	0,105	[82]
13,1	0,109	[83]
19	0,14	[84]

molecules. Conversion to the gas which is found in the pores of the structure is fairly simple, since the mean free path of the molecules is large in comparison with the sizes of the particles of the structure. Then one can consider such a system as a two-component gas; the gas molecules are one of its components, and the particles of the structure are the other. The mean free path of the molecules with respect to the particles of the structure equals:

$$\lambda' = (N' \cdot \pi r_0^2)^{-1} = 4/S\bar{\rho}, \tag{3.3}$$

where r_0 is the average radius of a structure particle, N' is the density of these particles, $\bar{\rho}$ is the mass density of the structure, and S is the specific area of the inner surface. The effective mean free path of a molecule with allowance for its collision with gas molecules and the structure equals

$$\lambda_{\text{eff}} = (1/\lambda + 1/\lambda')^{-1}.$$

Correspondingly, the expressions for the transfer coefficients are converted to the form:

$$\mathcal{D} = \frac{\mathcal{D}_{\text{fg}}}{1 + (\sqrt{2}\lambda/\lambda')}, \quad \eta = \frac{\eta_{\text{fg}}}{1 + (\lambda/\sqrt{2}\lambda')}, \quad \varkappa = \frac{\varkappa_{\text{fg}}}{1 + (\sqrt{2}\lambda/\lambda')}, \tag{3.4}$$

where $\mathcal{D}_{\text{fg}}$, η_{fg}, and $\varkappa_{\text{fg}}$ are the corresponding transfer coefficients that are attributed to a free gas.

Let us make estimates for an aerogel with density $\bar{\rho} = 0.01$ g/cm^3 and specific inner surface area $S = 1{,}000$ m^2/g, within which is found air at room temperature and atmospheric pressure. In this case we have $\lambda = 1.2 \cdot 10^{-5}$ cm and $\lambda' = 4 \cdot 10^{-5}$ cm, so that the coefficients of diffusion and thermal conductivity turn out to be approximately 30% lower than in free air, and the coefficient of viscosity is 15% lower than in air.

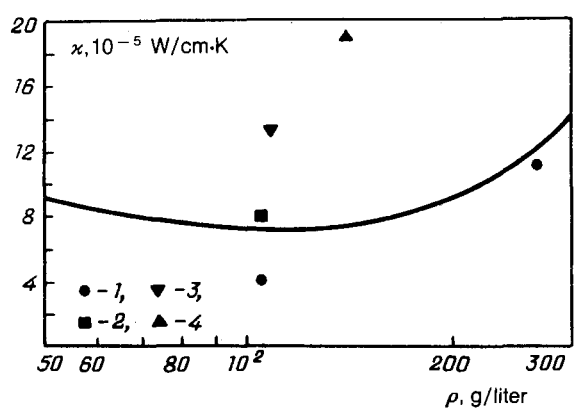

FIG. 3. The coefficient of thermal conductivity for silicon dioxide aerogel. The solid curve shows a calculation according to Eq. (3.5). Experimental data are from: *1*) Refs. 80 and 81; *2*) Ref. 82; *3*) Ref. 83; *4*) Ref. 84.

As far as thermal conductivity is concerned, there is another heat transfer channel corresponding to transport in the lattice of the structure. The contribution of this channel increases with increasing density of the structure. The existing information refers to silicon dioxide aerogel in the temperature range close to room temperature.[80–84] The results of the measurements conducted are collected in Table VI. Let us represent the dependence of the coefficient of thermal conductivity on aerogel density in the form $\varkappa \sim \rho^g$. The values of the exponent equal 1.6 according to Ref. 83 and 1.8 according to Ref. 85.

As is evident, heat transport through the lattice of the structure is significant at high densities of the structure, whereas at low densities heat transport occurs through the gas which is in the pores of the structure. Since these channels are independent, one may combine them, so that the total coefficient of thermal conductivity equals:

$$\varkappa = \frac{\varkappa_{\text{fg}}}{1 + (\sqrt{2}\lambda/\lambda')} + \varkappa_0 \left(\frac{\bar{\rho}}{\rho_0}\right)^g, \tag{3.5}$$

where $\varkappa_0$ and ρ_0 are parameters. Choosing $g = 1.7$ and $\rho_0 = 0.005$ g/cm^3, by processing the set of experimental data (see Table VI), we have $\varkappa_0 = (1.8 \cdot 10^{-5})(10^{\pm 0.3})$ W/cm·K. The dependence of the coefficient of thermal conductivity for a silicon dioxide aerogel on the aerogel density is shown in Fig. 3. For the chosen parameters, Eq. (3.5) gives a minimum for the coefficient of aerogel thermal conductivity almost four times smaller than its value in atmospheric air.[86]

A new mechanism of heat transfer in the structures under consideration that is associated with the vaporization and condensation of the molecules of the structure turns out to be significant at high temperatures. Let there be a temperature gradient ∇T in the system, and let us introduce the coefficient of thermal conductivity $\varkappa$ according to the relation

$$\mathbf{q} = -\varkappa \nabla T,$$

where q is the heat flux. Assuming that local thermodynamic equilibrium is maintained in the system, we have that the density of molecules at each point corresponds to the density $N(T)$ of the saturated vapor at a given temperature. Here $N(T) \sim \exp(-\varepsilon_a/T)$, where ε_a is the energy expended in vaporizing one molecule. The temperature gradient creates a gradient of the density of molecules, which equals

$$\nabla N = N \frac{\varepsilon_a}{T^2} \nabla T,$$

and this causes a flux of molecules $\mathbf{j} = \mathscr{D}\nabla N$, where $\mathscr{D}$ is the coefficient of molecular diffusion. Since each molecule transfers an energy ε_a which it returns to the particles of the structure upon condensation, then the thermal flux equals $\mathbf{q} = \varepsilon_a \mathbf{j}$. Comparing the expressions obtained, we have for the coefficient of thermal conductivity due to the mechanism under consideration:

$$\varkappa = \left(\frac{\varepsilon_a}{T}\right)^2 \mathscr{D} N(T). \tag{3.6}$$

We shall assume that the accommodation coefficient for the surface of the structure equals one, i.e., each collision of a vaporized molecule with the particles of the structure leads to condensation. Then the mean free path of a molecule is determined by Eq. (3.3), and the coefficient of thermal conductivity equals

$$\varkappa = \frac{3}{2} \cdot \left(\frac{\varepsilon_a}{T}\right)^2 \left(\frac{\pi T}{2M}\right)^{1/2} \frac{NT}{S\tilde{\rho}}, \tag{3.7}$$

where M is the mass of the molecules of which the structure consists.

The temperatures at which the mechanism of heat conduction under consideration becomes significant is of interest. Figure 4 shows the ratio of the coefficients of thermal conductivity for silicon dioxide aerogel that have been calculated according to Eqs. (3.7) and (3.4), and which are denoted as $\varkappa_7$ and $\varkappa_4$, respectively. Air at atmospheric pressure is found inside the aerogel. Here the coefficient $\varkappa_4$ is determined by the collisions of air molecules with the particles of the structure ($\rho \gtrsim 0.01$ g/cm^3). As is evident, the coefficients of thermal conductivity under consideration are comparable at a temperature near 1,900 K, and at the melting temperature the heat conduction through the vaporized molecules of the aerogel material is almost an order of magnitude larger than that by the action of the air molecules that are in the pores.

3.2. Combustion inside an aerogel

Thus, transport in macroscopic fractal systems differs somewhat from transport in a free gas. There is no convective transfer in such systems. The transfer which is achieved by the gas molecules is of the same nature as that in an ordinary gas, but its efficiency is lower, for along with the collisions between the gas molecules, this transport is determined by collisions of the molecules with the structure particles. These factors prolong the transport processes and can change their nature. Below, we shall demonstrate this for one of the examples, the combustion of charcoal inside an aerogel.

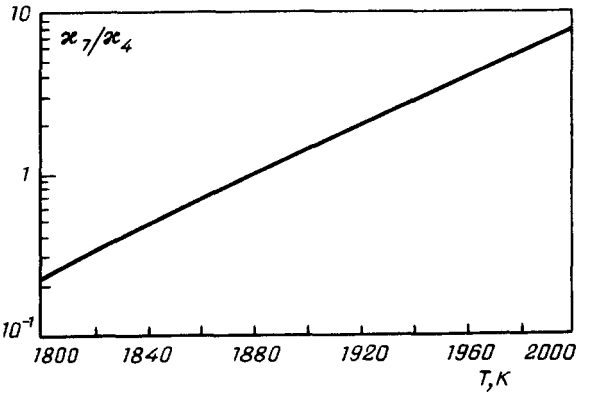

FIG. 4. The ratio of the coefficient of thermal conductivity for a silicon dioxide aerogel which corresponds to heat transfer by means of vaporized and condensed SiO_2 molecules to the coefficient of thermal conductivity determined by the transport of molecules.

Let us place a small piece of charcoal between two aerogel plates and heat it with a laser beam, bringing it to its ignition temperature. After this, let us turn off the laser and analyze the nature of combustion. The power of this process is determined by the rate of arrival of oxygen at the specimen, and the heat removal is connected with transport due to thermal conductivity and radiation of the specimen. As a specimen let us choose activated birch charcoal, for which the combustion parameters in the temperature range from 800 K to 1,800 K are well known.[87-90] Specifically, it burns through the entire volume of the specimen, and moreover, the specific power of the release of energy equals

$$Q = Q_0 \exp(-E_a/T),$$

where the activation energy $E_a = 34 \pm 1$ kcal/mole, and the factor in front of the exponential equals $Q_0 = (3 \pm 1) \cdot 10^{10}$ W/g.

Values of the temperature at which the thermal explosion of a specimen which is located inside a silicon dioxide aerogel occurs, and also the energy that is expended in heating the specimen to this temperature are shown in Table VII. The kinetic combustion parameters for activated charcoal were used to calculate the ignition temperature of the specimen.

After ignition, the specimen is heated to the temperature at which the power of release of energy is limited by the rate of oxygen arrival (the diffusion regime of combustion). This power of release of energy equals:

TABLE VII. Parameters of the combustion of an activated charcoal specimen inside silicon dioxide aerogel with 0.050 g/cm^3 density and 1,000 m^2/g specific inner surface.

Specimen radius, mm	0,2	0,4	0,8
Ignition temperature, K	990	940	890
Heating energy, J	0,01	0,09	0,6
Combustion temperature, K	1410	1220	1060
Contribution of heat conduction, %	14	10	7
Combustion time, sec	8	28	105
ξ	16	9	4

$$P_{\text{diff}} = 4\pi\mathcal{D}[O_2]R\varepsilon/(1-\beta),$$

where $\mathcal{D}$ is the diffusion coefficient of oxygen molecules, $[O_2]$ is the density of oxygen molecules far away from the specimen, R is the radius of the specimen, ε is the energy that is released by using one oxygen molecule, and $\beta = \mathrm{d}(\ln\mathcal{D}[O_2])/\mathrm{d}\ln T$ is a factor which allows for the temperature dependence of the flux of oxygen. Next we assume that carbon dioxide is the final product of combustion, i.e., $\varepsilon = 4.02$ eV, and the mean free paths of the molecules are independent of temperature, i.e., $\beta = 1/2$.

The power of the heat release is made up of two parts, which are due to radiation and heat conduction. Assuming the temperature far from the specimen to be low in comparison with the combustion temperature, we have for the radiation power

$$P_{\text{rad}} = 4\pi R^2 a\sigma T^4,$$

where σ is the Stefan–Boltzmann constant, and a is the grayness coefficient of the specimen. For an absolutely black body $a = 1$; we then assume $a = 0.8$ for activated charcoal. The power of the release of energy due to heat conduction equals

$$P_{\text{htc}} = 4\pi RT\varkappa(T)/(1-\alpha),$$

where $\alpha = \mathrm{d}\ln\varkappa/\mathrm{d}\ln T$. Assuming that the mean free path for molecules is independent of temperature, from now on we take $\alpha = -1/2$. Equating the heat release and heat removal powers, we find the combustion temperature, which is presented in Table VII together with the time for combustion (the density of activated charcoal is 0.8 g/cm^3) and the percentage of the energy losses that are expended due to the heat conduction of the gas. The coefficient ξ is the ratio of the powers of the release of energy at the combustion temperature and at the ignition temperature. This coefficient characterizes the margin of reliability of the result, since self-sustaining combustion is possible at $\xi > 1$.

The example considered shows features of the processes inside an aerogel. First, they are greatly slowed. Thus, a match burns in air for a time of the order of 10 sec. Since its supply of energy equals approximately 2 kJ, this corresponds to a 200 W power of release of energy. The last specimen in Table VII has a 50 J supply of energy, so that the power that is released during its combustion is lower by two and a half orders of magnitude than during the combustion of a match. Second, the main channel for heat removal inside an aerogel is due to radiation. A smaller part of the power that is dissipated is expended in radiation (including infrared) in flames created by the combustion of organic materials in air; this also includes those flames which are used as light sources.

One more small remark regarding the example considered. We implicitly assumed that the aerogel material is not destroyed at the combustion temperature of the specimen. Mechanisms for destroying an aerogel at high temperature will be considered later; this is connected with the densification of its structure. Going ahead, let us notice that the time for the densification of a silicon dioxide aerogel structure is one hour at the combustion temperature of the first specimen; in other cases, it is several orders of magnitude shorter. Thereby the combustion time of a specimen is several orders of magnitude shorter than the time for its destruction by heat.

4. FRACTAL SYSTEMS AS EXPLOSIVE MATERIAL

4.1. The supply of energy for fractal structures

The fractal systems under consideration consist of small sized particles. This is connected with the nature of the formation of these systems. The times of joining them into structures increase sharply with increasing particle size for all structure formation mechanisms. A small particle size in a structure corresponds to a large surface energy in the structure. Actually, a molecule which is located on the surface of a particle has half the number of bonds as a molecule located inside the particle. Therefore a reduction of the specific surface of a particle, in which certain specific surfaces of a molecule end up inside the material, is accompanied by the release of energy. Let us notice that, by its nature, the surface energy of fractal structures is chemical, for its release is connected with the formation of new chemical bonds.

The specific surface energy of structures equals $\eta\Delta H/2$, where η is the relative number of molecules which are located on the inner surface of a structure, and ΔH is the enthalpy of vaporization of the material of which the structure consists. Values of this for oxides of which aerogels may consist are 133 ± 7 kcal/mole for SiO_2, 133 ± 3 kcal/mole for CaO, and 136 ± 3 kcal/mole for TiO.[91] Accordingly, the specific surface energy divided by the mass of the surface molecules (i.e., $\Delta H/2$) is 4.6 kJ/g for SiO_2, 5.1 kJ/g for CaO, and 4.4 kJ/g for TiO. This energy is of the same order of magnitude as that for explosives, and it also has a chemical nature.

Let us find out what number of molecules are located on the inner surfaces of the structures under consideration. For simplicity, we shall assume that the structure consists of individual particles, small spheres of the same size. This will not lead to significant errors. For example, if one assumes that each sphere has three neighbors with which it is connected, and moreover, the radius of a "neck" in half the radius of a particle, then the area here is reduced by 20% in comparison with the case when the spheres are tangent to each other. Let us introduce the volume $a^3 = M/\rho_0$ which fits one molecule inside the material, so that M is the mass of a molecule, and ρ_0 is the specific mass of the material. Then we have for the relative number of molecules on the surface:

$$\eta = 1 - \left(\frac{r_0 - a}{r_0}\right)^3, \tag{4.1}$$

where r_0 is the average radius of the particles in the structure (actually, if $4\pi r_0^3/3$ is the total volume of a particle, then $4\pi(r_0 - a)^3/3$ is the volume that is occupied by the inner molecules).

Let us make specific estimates from this equation. Let us take a typical silicon dioxide aerogel with a 1,000 m^2/g specific area. We have $r_0 = 1.36$ nm, $a = 0.36$, i.e., $\eta = 0.60$ (the total number of molecules forming a particle in this case is about 230). From this we find the specific surface energy for the aerogel, which equals 2.8 kJ/g. This value is comparable with the specific energy of gunpowder.

Thus, the fractal structures are similar to explosives both in the type of internal energy, and also in its magnitude. Just as in gunpowders, the release of this energy may be accompanied by a thermal explosion. Next we shall consider

the kinetics of the process of releasing the surface energies of fractal clusters.

4.2. Energy release mechanisms in aerogels

A process of structure change leading to a reduction of the specific area of the inner surface occurs at high temperatures in aerogels. It is called the aerogel densification process. Its mechanisms consists of the following. The radiation of individual structure particles in a transparent aerogel leads to some decrease of the aerogel temperature in comparison with the temperature of the gas which is located in its pores. This temperature deviation is less for small particles of the structure than for large ones. Therefore the flux of molecules which are vaporized from the surfaces of small particles is greater than from the surfaces of the large ones. The condensation of vapor of the material onto particles of the structure leads to the large particles growing, and the small ones shrink and finally disappear. Thus, the reduction of the specific area of the inner surface of an aerogel is the result of this process.

Let us introduce the time τ for the process under consideration according to the equation:

$$dS/dt = -S/\tau, \tag{4.2}$$

where S is the specific area of the inner surface. One can reconstruct this value from the measurements by Mulder and van Lierop,[59] which have been carried out for a silicon dioxide aerogel in the 1,420 K to 1,500 K temperature range. In this experiment, the aerogel was placed in a thermostat with a specified temperature and was kept there for 12 minutes. The area of its inner surface was measured after this. Comparison of the data obtained with Eq. (4.2) enables one to determine the time for this process. The results are shown in Fig. 5. Let us notice that, according to the mechanism

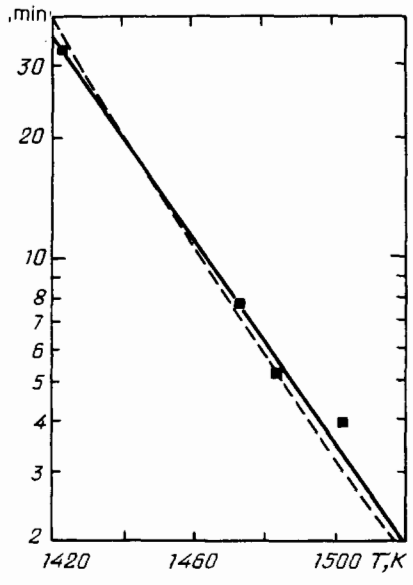

FIG. 5. The time for the densification process for a silicon dioxide aerogel. The symbols are experimental data from Ref. 59, the solid curve has been drawn from these values, and the dashed curve shows a calculation according to Eq. (4.3).

presented, the time for densifying an aerogel is determined by the equation

$$\tau = \tau_0 \exp(\Delta H/T), \tag{4.3}$$

where $\Delta H = 133 \pm 7$ kcal/mole[91] is the enthalpy of vaporization of the aerogel material. The calculation from Eq. (4.3) using $\tau_0 = 8 \cdot 10^{-18}$ sec as the factor in front of the exponential, which has been found on the basis of experimental data, is shown in Fig. 5. It is significant that the values of the activation energy for the aerogel densification process corresponding to experimental data and Eq. (4.3) agree within their accuracies. This fact confirms the mechanism presented for the aerogel densification process.

The rate of the aerogel densification process is determined by the difference of the fluxes of vaporization and condensation, which are almost equal. On the basis of the experimental data, let us compare this difference with the vaporization flux of material from the surface of a particle. Let us notice that the time for aerogel densification is introduced as

$$\frac{1}{\tau} = -\frac{d \ln S}{dt} = \frac{d \ln r_0}{dt}, \tag{4.4}$$

where r_0 is the average radius of the particles in the structure. Let us introduce the flux of vaporized molecules $j = N(T)\bar{v}/4$, where $N(T)$ is the density of molecules at the saturated vapor pressure corresponding to a given temperature,[92] and $\bar{v}$ is the mean thermal velocity of molecules. Let us assume that the accommodation coefficient equals one for collisions of molecules with the surface, i.e., a molecule, upon colliding with the surface of the material, sticks to it. For the number n of molecules in a particle with vaporization of molecules, occurring from the surface, we have:

$$\frac{dn}{dt} = -4\pi r_0^2 j.$$

The total number of molecules in a particle equals $n = 4\pi r_0^3 \rho_0/3M$, where ρ_0 is the density of the material, and M is the mass of an individual molecule. From this, we find

$$\frac{d \ln r_0}{dt} = -\frac{jM}{r_0 \rho_0}. \tag{4.5}$$

It is natural to assume that the rate of aerogel densification is proportional to the particle vaporization rate. This gives

$$\frac{1}{\tau} = C\frac{jM}{r_0 \rho_0}, \tag{4.6}$$

and moreover, in accordance with the nature of the process, $C \ll 1$. According to experimental data,[59] the value of this coefficient for silicon dioxide aerogel equals $C = 10^{-3.7 \pm 0.3}$.

Based on these data, let us make the following estimate. The aerogel densification process arises because the temperatures which correspond to the vaporization and condensation processes are somewhat different. The temperature dependences for the vaporization and condensation fluxes have the form $j \sim \exp(-\Delta H/T)$, where ΔH is the enthalpy of vaporization of the material. From this, we find for the difference of the effective temperatures of vaporization and condensation in an aerogel:

$$\Delta T = CT^2/\Delta H.$$

In particular, for a silicon dioxide aerogel at $T = 1{,}500$ K temperature, which corresponds to the experiment under consideration, the effective temperature difference which applies to vaporization and condensation equals $\Delta T = 0.07$ K. If, in accordance with the mechanism under consideration, one assumes that the temperature of a particle depends on its radius, then $\Delta t = r(dT/dr)$ and the temperature gradient in the case under consideration equals $dT/dr \approx 0.04$ K/nm. Let us note that this value depends on the transparency of the material, and for other ceramics that are used as aerogel material, one must expect larger values of the temperature gradient. Here the connection between the time for structure densification and the system parameters is given by the equation

$$\frac{1}{\tau} = \frac{jM}{\rho_0} \cdot \frac{\Delta H}{T^2} \cdot \frac{dT}{dr}. \tag{4.7}$$

Another densification mechanism occurs at temperatures above the melting temperatures of the material. Then the structure is breaking up into a set of independent liquid drops, and the process of structure densification is determined by coagulation, the joining of drops into larger sized drops upon collision. Assuming that drops are joined upon each contact and that their contact occurs upon direct collision, we have the following expression for the constants of the rate of joining drops of radii r_1 and r_2:

$$k = \left[\frac{8T(m_1 + m_2)}{\pi m_1 m_2}\right]^{1/2} \pi(r_1^2 + r_2^2), \tag{4.8}$$

where m_1 and m_2 are the masses of particles of radii r_1 and r_2. The joining of these drops leads to the reduction of the area of their total surfaces by the amount $4\pi(r_1^2 + r_2^2) - 4\pi(r_1^3 + r_2^3)^{2/3}$. Therefore, the equation for the specific area of a surface takes the form:

$$\frac{dS}{dt} = -4\pi N(8T\pi)^{1/2}\left\langle\left(\frac{m_1 + m_2}{m_1 m_2}\right)^{1/2} \times \frac{(r_1^2 + r_2^2)[r_1^2 + r_2^2 - (r_1^3 + r_2^3)^{2/3}]}{(m_1 + m_2)}\right\rangle,$$

where N is the particle density, and the triangular brackets denote averaging with respect to mass over the particle distribution.

We shall assume for simplicity that the distribution function of particles with respect to mass has the form $f(m) \sim \exp(-m/\bar{m})$, where $\bar{m} = (4/3)\pi r_0^3 \rho_0$ is the average mass of a particle and ρ_0 is the density of its material. Then one can represent the equation for the evolution of the specific area of the surface of a particle in the form

$$\frac{dS}{dt} = -S\left(\frac{6Tr_0}{\rho_0}\right)^{1/2} NJ, \tag{4.9}$$

where

$$J = \int_0^\infty dx \int_0^\infty dy \exp(-x - y)[xy(x + y)]^{-1/2}[x^{2/3} + y^{2/3} - (x + y)^{2/3}] = 0{,}61.$$

Let us solve this equation, considering that the average particle density is $N \sim r_0^{-3}$ and the specific area of a surface is $S \sim 1/r_0$. We shall find

$$S = S_0/\left[1 + (5\nu_0 t/2)\right]^{0.4}, \tag{4.10}$$

where S_0 is the specific particle surface area at the initial time, $\nu_0 = 1.5(\mathrm{Tr}_0/\rho_0)^{1/2} N_0$, and N_0 is the initial particle density.

Let us notice that triggering of the structure densification mechanism under consideration sharply accelerates this process. For example, in the case of a silicon dioxide aerogel with 0.01 g/cm^3 density and a specific inner surface area of 1,000 m^2/g, according to Eq. (4.3) the time for structure densification of solid aerogel near the melting point equals $\tau = 0.003$ sec. The time for changing the surfaces of liquid particles is $1/\nu_0 = 1.8 \cdot 10^{-8}$ sec. Another remark pertains to the protraction of the structure densification process in the case of liquid particles. For example, according to Eq. (4.10), 20% of the surface energy is released after a time $0.3/\nu_0$, 80% of the internal energy is released after time $22/\nu_0$, and 90% of the internal energy is released after time $130/\nu_0$.

5. THERMAL EXPLOSION AND THE PROPAGATION OF A THERMAL WAVE IN STRUCTURES

5.1. The threshold for thermal explosion

A thermal explosion in a system occurs at conditions[93,94,95] when the heat release increases sharply (exponentially) with temperature, and the heat removal depends smoothly on it. Then conditions may arise when a small change of the system temperature is not compensated for by heat removal, but leads to an acceleration of thermal processes in the system and causes its subsequent heating. The development of these processes leads to a thermal explosion, as a result of which either the entire energy released remains inside the system and heats it, or the system goes over into another regime in which other heat removal mechanisms operate at higher temperatures.

One of such examples was considered earlier in Subsection 3.2. A charcoal specimen which is located inside an aerogel is heated by laser action and, at a definite temperature, a thermal explosion occurs which causes the specimen to start burning. Then it is heated and burns under the action of internal processes which are responsible for combustion of the specimen by use of the oxygen which reaches it.

Next we shall consider an extension of this example. We shall raise the temperature of the specimen further as long as the process of aerogel densification does not enter into play. At a definite temperature the heat conduction flux from the specimen will be provided due to heat release because of the aerogel densification process near the specimen. Then the process can be maintained due to the internal energy of the aerogel. The region near the specimen being heated is heated to such a temperature which can supply the internal energy of the aerogel, and the region being heated will be propagated through the entire aerogel, i.e., a thermal explosion will occur. The relation between the radius of the region being heated and the threshold temperature for a thermal explosion for a silicon dioxide aerogel with $\rho = 0.01$ g/cm^3 density and $S = 1{,}000$ m^2/g specific inner surface area is presented in Fig. 6. In accordance with the mechanism of the

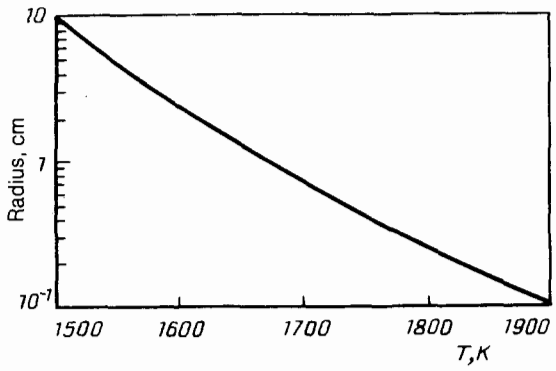

FIG. 6. The radius of a sphere which is located inside a silicon dioxide aerogel. Upon heating the sphere to the indicated temperature, a thermal explosion of the aerogel occurs.

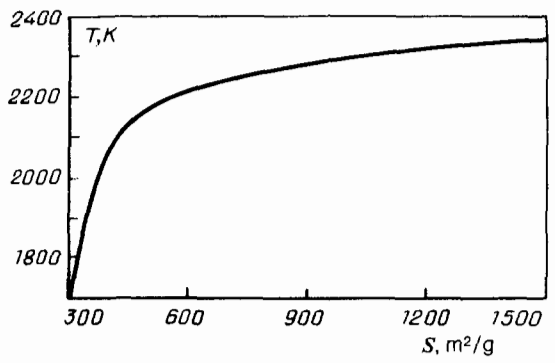

FIG. 7. The maximum temperature that is reached during a thermal explosion in a silicon dioxide aerogel.

aerogel densification process, a thermal explosion of the aerogel is observed at high temperatures.

These estimates can have practical importance. Aerogel is used in large quantities in accelerators as a material for one of the types of Cherenkov detectors. For example, 1,700 liters of aerogel has been used in one of the first devices of this type in the DESY accelerator (Hamburg).[59,99,100] Silicon dioxide aerogel is similar to glass in its external form, and it evidently evokes just such an impression in specialists in considering safety problems. However, it is evident from the estimates presented that it will behave like an explosive at high temperatures. In particular, it follows from this that hundreds of kilograms of an explosive have been deposited at the Hamburg accelerator, which could explode during a fire. It is clear that understanding this fact will enable one to avoid much unpleasantness.

It is evident that the explosion which occurred at the Swedish "Aeroglass" firm that produced silicon dioxide aerogel for the Cherenkov detectors of an accelerator at CERN was related to this.[101,102,103] More than 1,000 liters of aerogel were produced in 1979, and moreover, a facility with a 98 liter volume was used, in which 270 °C temperature and 90 bars pressure were released (the critical temperature and pressure for methyl alcohol are 240 °C and 78.5 bars, respectively). 18 pieces of aerogel of 20 cm × 20 cm × 3 cm size (a volume larger than 20 liters) were produced at one time. Then a new facility with a 1,100 liter volume was constructed, in which 100 pieces of aerogel of 60 cm × 50 cm × 2 cm (a 360 liter volume) could be produced at one time. After several successful batches of aerogel were produced, a leak of methyl alcohol occurred on August 27, 1984, which led to an explosion. As a result, the building in which the facility was housed was destroyed, and three people who were in it were injured. A special investigation revealed neither errors by the staff nor failure of technology. In the scheme of the estimates made above, one may suppose that a leak of methyl alcohol caused a fire to start and heated the aerogel, which then led to a powerful explosion.

5.2. A thermal wave in an aerogel

The occurrence of a thermal explosion is accompanied by the propagation of a thermal wave in the specimen. Estimating the parameters of the thermal wave is our next problem. Since this process proceeds relatively fast, at first all the energy that is released remains inside the specimen and leads to its heating, melting, and partial vaporization. Thereby, the temperature behind the thermal wave front is determined by the internal energy. For the structure densities under consideration ($\rho \sim 0.01$ g/cm^3), the gas which is located inside it affects the thermal balance of the system only slightly. The part of the material which was vaporized plays a definite role at high temperatures. The dependence of the maximum temperature of the system on the specific inner surface area (or on the average particle radius for the structure) is given in Fig. 7. The calculation has been made for silicon dioxide aerogel. It was assumed that the specific heat of silicon dioxide, which equals 0.75 J/g·K at room temperature,[91] is independent of temperature. Let us notice that the specific inner surface areas of actual silicon dioxide aerogel specimens are in the range from 500 m^2/g to 1,500 m^2/g.

Next, finding the velocity of a thermal wave in aerogel is our problem. Let us determine this characteristic by an approximate method based on the Zel'dovich–Frank-Kamenetskiĭ theory.[94,96] Since the temperature dependences of the parameters of the problem are different from the traditional ones in the high-temperature range, certain elements of this theory will be discussed. The equation for the temperature in the wave has the form:

$$\rho c_p \frac{\partial T}{\partial t} = \frac{Q\bar{\rho}}{\tau} + \varkappa \frac{\partial^2 T}{\partial x^2}; \tag{5.1}$$

here x is the direction of wave propagation, c_p is the specific heat of the structure, $\bar{\rho}$ is its density, Q is the specific supply of energy, τ is the time for the release of energy, and $\varkappa$ is the coefficient of thermal conductivity. Assuming that the wave propagates to the right, we find that all its characteristics depend on the argument $x-ut$, where u is the thermal wave velocity. Accordingly, Eq. (5.1) is reduced to the form

$$-u \frac{dT}{dx} = f + \chi \frac{d^2 T}{dx^2}, \tag{5.2}$$

where $f = Q/(c_p \tau) = T_m/\tau$, and $\chi = \varkappa/(c_p \bar{\rho})$ is the thermal conductivity of the system (T_m is the maximum temperature in the wave).

Following the Zel'dovich–Frank-Kamenetskiĭ theory, let us introduce the new variable $Z = -dT/dx$, and by means of it let us obtain the first order non-linear equation:

$$-uZ + \chi Z dZ/dT + f(T) = 0. \tag{5.3}$$

If the maximum temperature T_m in the wave is lower than the melting temperature and is located in a region where χ depends only slightly on temperature, one may use the traditional solution of the equation. In the range of temperatures $T_m - T \gg T^2/E_a$, one may neglect the last term in the equation, and its solution has the form $Z = u\int_{T_0}^{T} dT'/\chi$, where T_0 is the initial temperature. In the range of temperatures $T_m - T \ll T - T_0$, we neglect the first term of the equation. Joining the solutions, we shall obtain the Zel'dovich–Frank-Kamenetskiĭ equation for the thermal wave velocity:

$$u = (2\int_{T_0}^{T_m} dT'/\chi)^{1/2}/(\int_{T_0}^{T_m} dT'/\chi). \tag{5.4}$$

The lower limit of integration in the first integral is chosen so that the integral is independent of it. Taking into account that, in accordance with Eqs. (3.1), $\chi \sim T^{-1.2}$, and $\tau(T) \sim \exp(-E_a/T)$, we have the following expression for the thermal wave velocity in this case

$$u = \left(\frac{8}{9}\cdot\frac{T_m}{E_a}\cdot\frac{\chi(T_m)}{\tau(T_m)}\right)^{1/2} \tag{5.5}$$

As the temperature increases, the wave velocity has break points in two regions. The first of them corresponds to the temperature where a new heat conduction mechanism connected with the transport of molecules which are being vaporized and condensed becomes significant (see Subsection 3.1). This temperature equals $T_1 = 1{,}880$ K for a silicon dioxide aerogel. After passing through this point, the increase of the wave velocity with increasing maximum temperature slows down. This is connected with the triggering of a new heat conduction mechanism due to the vaporization and condensation of the molecules of the material, which causes an exponential increase of the coefficient of thermal conductivity with temperature.

The other region of the change of the temperature dependence of the thermal wave velocity starts at the melting point of the structure T_{mp} ($T_{mp} = 1{,}993$ K for silicon dioxide[92]), at which the mechanism of the densification process changes so that the rate of this process increases by several orders of magnitude. Upon passing through the melting temperature, the velocity of a thermal wave in a silicon dioxide aerogel increases by almost two orders of magnitude.

The calculation of the thermal wave velocity may be completely standard with allowance for the indicated features. Let us present this solution for temperatures higher than the melting temperature. One may neglect the last term of Eq. (5.3) in the $T < T_{mp}$ range and, by virtue of the sharp increase with temperature of the coefficient of thermal conductivity at $T > T_1$, this range does not make a contribution to the integral of Z. This gives $Z = 1.5uT_1/\chi_0(T_1)$, where the coefficient of thermal conductivity χ_0 is determined only by the transport of gas molecules inside the structure.

In the $T > T_{mp}$ range we neglect the first term of Eq. (5.3) and allow for the exponential dependence of the coefficient of thermal conductivity χ on temperature. Then, for $T_m - T_{mp} \gg \Delta T = T_{mp}^2/E_a$ ($\Delta T = 60$ K for silicon dioxide), we have

$$Z = \left[\frac{2\nu(T_{mp})T_m T_{mp}^2}{E_a \chi(T_{mp})}\right]^{1/2},$$

where $\nu(T_{mp})$ is the frequency of the change of the specific surface for the structure particles at the melting temperature. Obviously $\nu(T_{mp}) = \nu_0$, so that, by joining the solutions, we have for the thermal wave velocity

$$u = \frac{T_{mp}}{T_1}\cdot\left(\frac{8}{9}\cdot\frac{T_m}{E_a}\cdot\frac{\nu_0\chi_0^2(T_1)}{\chi(T_{mp})}\right)^{1/2}. \tag{5.6}$$

This is the asymptotic value which the thermal wave velocity approaches at high temperatures ($u \sim T_m^{1/2}$). For silicon dioxide aerogel with $\rho = 0.01$ g/cm^3, this value equals $u \approx 80$ cm/sec ($T_m = 2{,}400$ K). The temperature dependence of the velocity of a thermal wave propagating in a silicon dioxide aerogel whose density equals $\rho = 0.01$ g/cm^3 is given in Fig. 8.

5.3. A thermal wave along a fractal fiber

The propagation of a thermal wave along a fractal fiber apparently has a direct relation to ball lightning. Actually, an analysis of the properties of ball lightning that have been obtained by observing it shows that a fractal structure is the most acceptable structure for ball lightning.[5,53,97,98] Electrical processes in the atmosphere which are accompanied by the vaporization of materials can lead to the formation of a large number of fractal fibers. A small ball of these fibers makes up the framework of ball lightning, and thermal waves which propagate simultaneously along different fractal fibers create the luminescence of ball lightning. This model requires detailed analysis and the performance of modeling experiments for the purpose of understanding details of the processes; however, the general scheme does not contradict either the observational data not scientific ideas and information concerning individual processes.

Let us consider the features of a thermal wave propagating along a fractal fiber. The regularities which apply to an aerogel obviously remain valid in this case, but there appear additional factors which arise because a fractal fiber has a separation boundary. In the case of an aerogel, an isotropic system of large dimensions, a thermal wave propagates from

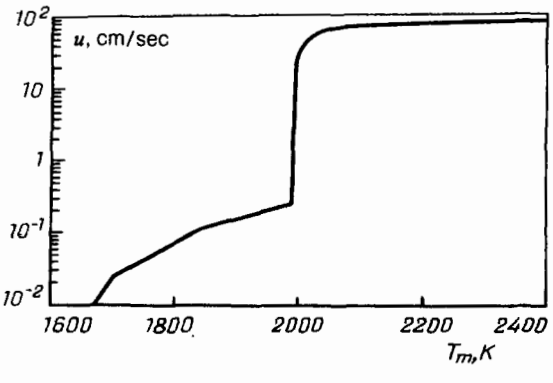

FIG. 8. The velocity of a thermal wave in silicon dioxide aerogel as a function of the maximum temperature in the wave.

a certain region in all directions, so that the process itself is a thermal explosion. In the case of a fractal fiber, the wave moves in one direction, along the fiber, and processes which go on in the gas at the boundary of the fiber affect it.

The most important among them is heat removal due to the heat conduction of the gas surrounding the fractal fiber. This process cal lead to a reduction of the maximum temperature of the wave, and causes a temperature drop behind the wavefront (see Fig. 9). Besides, it creates an additional condition for the existence of a thermal wave which is absent in the case of an aerogel. Specifically, the characteristic time for heat removal must be much longer than the characteristic time for the thermal process inside the wave. Otherwise, the internal energy of the system cannot be used in a thermal wave.

Let us make suitable estimates for a silicon dioxide fractal fiber. The thermal flux caused by the heat conduction of gas equals

$$q = \frac{T\varkappa(T)}{(\alpha + 1)R\ln(l/R)},$$

where $\varkappa$ is the coefficient of thermal conductivity of the gas, $\alpha = \mathrm{d}\ln\varkappa/\mathrm{d}\ln T$, R is the fiber radius, and l is the length of the heated section ($l \gg R$). Assuming that the density of the fiber equals 0.01 g/cm^3, the specific inner surface area $S = 1{,}000$ m^2/g, the radius $R = 20$ μm, and $l/R = 10$, we shall find for the characteristic time for cooling $\tau_{\mathrm{col}} = 0.0001$ sec to 0.0002 sec in the temperature range from 1,600 K to 2,000 K. Since the time for the process of structure densification is $\tau = 0.003$ sec for a solid fiber at the melting point of the material, one can draw the conclusion from this that a thermal wave does not exist if the fractal fiber is not melted behind the wavefront. As a result of melting of the structure and its breakup into individual drops, the mechanism for increasing the specific inner surface of the structure changes, and the condition under consideration for the existence of the wave is fulfilled. Then wave propagation velocity in a fractal fiber is the same as in an aerogel, and the size of the hot, luminous zone behind the wave is $l \sim u\tau_{\mathrm{col}} \sim 0.01$ cm. The width of the leading front in this case is of the order 0.1 μm to 1 μm.

Under consideration at the same time is the condition imposed on the specific internal energy of the system: the processing of this energy must lead to melting of the specimen. Thereby, it is necessary for the existence of a wave that the specific inner surface area exceed a certain amount. In particular, for silicon dioxide this amount is about 400 m^2/g. Therefore, this condition is certainly fulfilled for aerogel material located on an active surface for specimens obtained by the electrical explosion of a wire, and is evidently not filled for specimens obtained by laser vaporization of the material.

Let us point out the features of a thermal wave being propagated along a fractal fiber. Since the fiber density is approximately two orders of magnitude higher than the density of air, cooling of the fiber material starts when the size of the heated region significantly exceeds the fiber size. Actually, the size of the hot, luminous region near the fiber amounts to a fraction of a millimeter. Another feature is connected with the escape of vaporized molecules of fiber material beyond it. At high temperatures in a thermal wave, when the vapor of the molecules makes a contribution to the specific heat of the system, the departure of vaporized molecules beyond the fiber and their condensation far from the fiber show up in the nature of heat removal and the nature of the luminescence of the heated region.

Thus, the velocity of a thermal wave propagating in a fractal fiber is the same as in an aerogel in the case that the structure behind the thermal wavefront is melted. Otherwise, a thermal wave does not exist, for the densification of solid structure takes a relatively long time and does not allow transport of the energy that is released along the fiber.

Let us pause for one more aspect of the process under consideration. Because of the high temperature at a thermal wavefront, liquid particles of the structure radiate efficiently, so that the system under consideration may be an efficient light source. Values of the light output of such a system as a function of the maximum temperature in the wave are shown in Fig. 10 to estimate this property. These calculations are based on the same parameters for a fractal fiber that were used earlier; however, a large uncertainty is contained in the

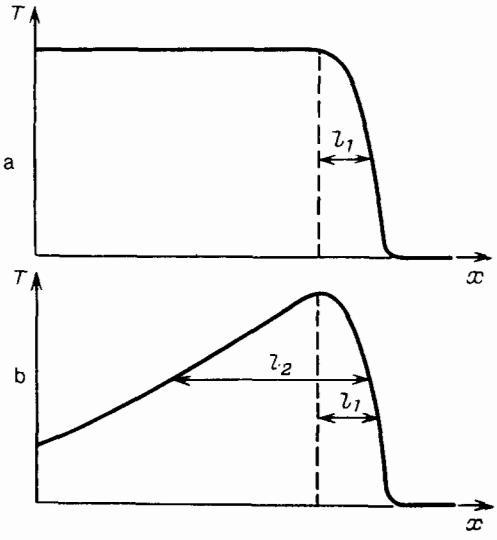

FIG. 9. Temperature distribution in the direction of thermal wave propagation a) in an aerogel and b) along a fractal fiber.

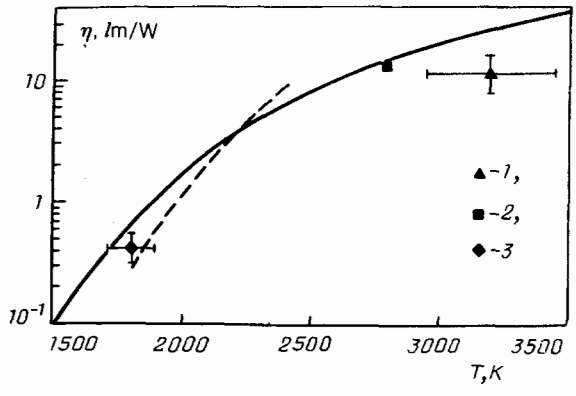

FIG. 10. The light output of some light sources. The solid curve shows an absolutely black body; the dashed curve shows a fractal fiber; *1*) shows pyrotechnic compounds; *2*) shows an electric lamp; and *3*) shows a candle flame.

optical properties for a particle of the material. This uncertainty increases for transparent materials such as silicon dioxide, for their transparency is lost at high temperatures. The optical parameters of soot at room temperature were used in making the calculation for the particles of the hot region of the thermal wave. Here tens of percent of the internal energy are used up for radiation in the temperature range under consideration. This system has more favorable radiation spectrum than an absolutely black body, and therefore the light output of a transparent hot region can exceed the light output of an absolutely black body if a significant part of the energy that is released is used up for radiation. For the conditions under consideration, the optical depth of a hot region for the visible spectral range is of the order of one. The hot region of the thermal wave is transparent to the infrared part of the spectrum, which makes the main contribution to the radiative power.

6. CONCLUSION

The analysis that has been carried out shows that macroscopic fractal structures possess high surface energies and can release this energy in a thermal explosion, which is accompanied by the propagation of a thermal wave. The characteristics of fractal systems for these processes are that these processes can go on only at relatively high temperatures. This feature of fractal systems can be used in special equipment and requires more attentive study of the properties being considered of these materials.

[1]F. Family and D. P. Landau (Eds.) *Kinematics of Aggregation and Gelation*, North-Holland, Amsterdam, 1984.
[2]H. E. Stanley and N. Ostrowsky (Eds.), *On Growth and Form*, Martinus Nijhoff, The Hague, 1985.
[3]H. J. Herrmann, Phys. Rep. **136**, 155 (1986).
[4]L. M. Sander, Nature **322**, 789 (1986).
[5]B. M. Smirnov, Usp. Fiz. Nauk **149**, 177 (1986) [Sov. Phys. Usp. **29**, 481 (1986)].
[6]S. H. Liu, Solid State Phys. **39**, 206 (1986).
[7]L. Pietronero and E. Tosatti (Eds.), *Fractals in Physics*, North-Holland, Amsterdam, 1986.
[8]L. M. Sander and M. E. Cates, Science **232** (1986).
[9]R. Jullien and R. Botet, *Aggregation and Fractal Aggregates*, World Scientific, Singapore, 1987.
[10]P. Meakin, Crit. Rev. Solid State Mater. Sci. **13**, 143 (1987).
[11]R. Jullien, L. Peliti, R. Rammal, and N. Bocara (Eds.), *Universalities in Condensed Matter*, Springer-Verlag, Berlin, Heidelberg, New York, 1988.
[12]D. P. Landau, K. K. Mon, and H. B. Schuttler (Eds.), *Computer Simulation Studies in Condensed Matter Physics*, Springer-Verlag, Berlin; Heidelberg; New York, 1988.
[13]T. Vicsek, *Fractal Growth Phenomena*, World Scientific, Singapore, 1987.
[14]B. M. Smirnov, Phys. Rep. **188**, 1 (1990).
[15]B. M. Smirnov, *Physics of Fractal Clusters* (In Russian), Nauka, M., 1991.
[16]S. R. Forrest and T. A. Witten, J. Phys. A **12**, L109 (1979).
[17]C. G. Granqvist and R. A. Buhrman, J. Appl. Phys. **47**, 2200 (1976).
[18]G. A. Niklasson *et al.*, Bull. Am. Phys. Soc. **28**, 528 (1983).
[19]G. A. Niklasson, S. Yatsuya, and C. G. Granqvist, Solid State Commun. **59**, 579 (1986).
[20]G. A. Niklasson and C. G. Granqvist, Phys. Rev. Lett. **56**, 256 (1986).
[21]G. A. Niklasson *et al.*, J. Appl. Phys. **62**, 259 (1987).
[22]G. A. Niklasson, A. Torebring, C. Larsson, and C. G. Granqvist, Phys. Rev. Lett. **60**, 1735 (1988).
[23]A. A. Lushnikov, A. V. Pakhomov, and G. A. Chernyaeva, Dokl. Akad. Nauk SSSR **292**, 86 (1987) [Sov. Phys. Dokl. **32**, 45 (1987)].
[24]A. A. Lushnikov, V. V. Maksimenko, and A. V. Pakhmov, J. Aerosol Sci. **20**, 865 (1989).
[25]F. V. Bunkin, N. A. Kirichenko, and B. V. Luk'yanchuk, Usp. Fiz. Nauk **138**, 45 (1982) [Sov. Phys. Usp. **25**, 662 (1982)].
[26]F. V. Bunkin, N. A. Kirichenko, and B. V. Luk'yanchuk, Izv. Akad. Nauk SSSR Ser. Fiz. **47**, 2000 (1983) [Bull. Acad. Aci. USSR Phys. Ser. **47**, No. 10, 115 (1983)]; Izv. Akad. Nauk SSSR Ser. Fiz. **48** (1984) [Bull. Acad. Sci. USSR Phys. Ser. **48**, No. 8, 27 (1984)]; Izv. Akad. Nauk SSSR Ser. Fiz. **49**, 1054 (1985) [Bull. Acad. Sci. USSR Phys. Ser. **49**, No. 6, 13 (1985)].
[27]A. J. Hurd, D. W. Schaefer, and J. E. Martin, Phys. Rev. A **35**, 2361 (1987).
[28]J. Turkevich, P. Stevenson, and J. Hiller, J. Am. Chem. Soc. **11**, 55 (1951).
[29]P. Meakin, Phys. Rev. Lett. **51**, 11 (1983).
[30]M. Kolb, R. Botet, and R. Jullien, Phys. Rev. Lett. **51**, 1123 (1983).
[31]M. Kolb and R. Jullien, J. Phys. (Paris) **45**, L977 (1984).
[32]R. Jullien and M. Kolb, J. Phys. A **17**, L639 (1984).
[33]R., Jullien, M. Kolb, and R. Botet, J. Phys. A **17**, L75 (1984).
[34]W. D. Brown and R. C. Ball, J. Phys. A **18**, L517 (1985).
[35]D. Weitz and M. Oliveria, Phys. Rev. Lett. **52**, 1433 (1984).
[36]K. D. Keefer and D. W. Schaefer, Phys. Rev. Lett. **56**, 2376 (1986).
[37]D. A. Weitz *et al.*, Phys. Rev. Lett. **53**, 1657 (1984).
[38]D. W. Schaefer *et al.*, Phys. Rev. Lett. **52**, 2371 (1984).
[39]D. W. Schaefer and K. D. Keefer, Phys. Rev. Lett. **53**, 1383 (1984).
[40]D. A. Weitz *et al.*, Phys. Rev. Lett. **54**, 1416 (1985).
[41]C. Aubert and D. S. Cannell, Phys. Rev. Lett. **56**, 738 (1986).
[42]P. Dimon *et al.*, Phys. Rev. Lett. **57**, 595 (1986).
[43]J. E. Martin, Phys. Rev. A **36**, 3415 (1987).
[44]P. W. Rouw, *Adhesive Hard Sphere Dispersion*, Doctoral Dissertation, Van't Hoff Laboratory, University of Utrecht, Holland, 1988.
[45]P. Wiltzius, Phys. Rev. Lett. **58**, 710 (1987).
[46]H. M. Lindsay, R. Klein, D. A. Weitz *et al.*, Phys. Rev. A **38**, 2614 (1988).
[47]G. Bolle, C. Cametti, P. Codastefano, and P. Tartaglia, Phys. Rev. A **35**, 837 (1987).
[48]C. Cametti, P. Codastefano, and P. Tartaglia, Phys. Rev. A **36**, 4916 (1987).
[49]J. P. Wilcoxon, J. E. Martin, and D. W. Schaefer, Phys. Rev. A **39**, 2675 (1989).
[50]J. E. Martin, D. W. Schaefer, and A. J. Hurd, Phys. Rev. A **33**, 3540 (1986).
[51]Y. Kantor and T. A. Witten, J. Phys. (Paris) **45**, L675 (1984).
[52]J. Fricke (Ed.), *Aerogels*, Springer-Verlag, Berlin, Heidelberg, New York, 1986.
[53]B. M. Smirnov, Usp. Fiz. Nauk **152**, 133 (1987) [Sov. Phys. Usp. **30**, 420 (1987)].
[54]J. Fricke, Scientific American **258**, No. 5, 92 (1988) [Russ. Transl., V. mire nauki No. 8, 50 (1988)].
[55]G. Poelz, in *Aerogels* (J. Fricke, Ed.), Springer-Verlag, Berlin, Heidelberg, New York, 1986, p. 176.
[56]S. S. Kistler, J. Phys. Chem. **34**, 52 (1932); **46**, 19 (1942).
[57]S. S. Kistler and A. G. Cadwell, Indust. Eng. Chem. **26**, 658 (1934).
[58]S. S. Kistler, J. Chem. Phys. **39**, 79 (1935).
[59]C. A. M. Mulder and J. G. van Lierop, in *Aerogels* (J. Fricke, Ed.), Springer-Verlag, Berlin, Heidelberg, New York, 1986, p. 68.
[60]F. J. Broeckner, W. Heckmann, F. Fisher *et al.*, in *Aerogels* (J. Fricke, Ed.), Springer-Verlag, Berlin, Heidelberg, New York, 1986, p. 176.
[61]D. W. Schaefer and K. D. Keefer, Phys. Rev. Lett. **56**, 2199 (1986).
[62]R. Vacher, T. Woignier, J. Pelous, and E. Courtens, Phys. Lett. B **37**, 6500 (1988).
[63]E. Courtens, R. Vacher, J. Pelous, and T. Woignier, Europhys. Lett. **6**, 245 (1988).
[64]R. Vacher, E. Courtens, G. Coddens, J. Pelous, and T. Woignier, Phys. Lett. B **39**, 7384 (1989).
[65]E. Courtens, R. Vacher, and E. Stoll, Physica Ser. D **38**, 41 (1989).
[66]R. Vacher, E. Courtens, G. Coddens, A. Heidemann *et al.*, Phys. Rev. Lett. **65**, 1008 (1990).
[67]T. Freltoft, J. K. Kjems, and D. Richter, Phys. Rev. Lett. **59**, 1212 (1987).
[68]G. Reichenauer, J. Fricke, and U. Buchenau, Europhys. Lett. **8**, 415 (1989).
[69]H. Conrad, U. Buchenau, R. Schatzler *et al.*, Phys. Rev. B **41**, 2573 (1990).
[70]D. W. Schaefer, C. J. Brinker, D. Richter *et al.*, Phys. Rev. Lett. **64**, 2316 (1990).
[71]T. Freltoft, J. K. Kjems, and S. K. Sinha, Phys. Rev. B **33**, 269 (1986).
[72]A. A. Lushnikov, A. Negin, and A. V. Pakhomov, in *Sharovaya Molniya (Ball lightning*, B. M. Smirnov, (Ed.)), IVTAN SSSR, M. (1990), p. 11; Chem. Phys. Lett. **175**, 138 (1990).
[73]V. Ya. Aleksandrov, I. P. Borodin, E. V. Kichenko, and I. V. Podmoshenskiĭ, Zh. Tekh. Fiz. **52**, 818 (1982) [Sov. Phys. Tech. Phys. **27**, 527 (1982)].
[74]B. M. Smirnov, in *Trends in Physics; Book of Abstracts of the Eighth General Conference of The European Physical Society* (F. Pleiter, Ed.) North-Holland, Amsterdam, 1990, p. 83.
[75]B. M. Smirnov, Teplofiz. Vys. Temp. **29**, 418 (1991) [High Temp. **29** (1991)].

[76]P. Meakin and R. Jullien, J. Chem. Phys. **89**, 246 (1988).
[77]P. Meakin, J. Chem. Phys. **83**, 3645 (1985).
[78]S. Chapman and T. G. Cowling, *Mathematical Theory of Non-Uniform Gases*, 3rd edition, Cambridge Univ. Press, Cambridge, England (1970) [Russ. transl. of 2nd ed. IL, M., 1960]).
[79]J. H. Ferziger and H. G. Kaper, *Mathematical Theory of Transport Processes in Gases*, North-Holland, Amsterdam, 1972 [Russ. transl., Mir, M. 1976].
[80]J. Fricke (Ed.), *Aerogels*, Springer-Verlag, Berlin, Heidelberg, New York, 1986, p. 2.
[81]R. Caps and J. Fricke, in *Aerogels* (J. Fricke, Ed.), Springer-Verlag, Berlin, Heidelberg, New York, 1986, p. 110.
[82]D. Buttner and J. Fricke, The Physics Institute, University of Würzburg, Report E12-0784-1 (1984).
[83]O. Nilsson, A. Fransson, and J. Sandberg, in *Aerogels* (J. Fricke, Ed.) Springer-Verlag, Berlin, Heidelberg, New York, 1986, p. 121.
[84]M. Rubin and C. M. Lampert, Solar Energy Mater. 7, 393 (1983).
[85]D. Buttner, E. Hummer and J. Fricke, in *Aerogels* (J. Fricke, Ed.) Springer-Verlag, Berlin, Heidelberg, New York, 1986, p. 116.
[86]N. B. Vargaftik, *Tables on the Thermophysical Properties of Liquids and Gases*, 2nd ed., Halsted Press, N.Y., 1975 [Russ. original, Nauka, M., 1972 and Energoatomizdat, M., 1990].
[87]I. W. Smith and R. J. Tyler, Fuel **51**, 312 (1972).
[88]I. W. Smith and R. J. Tyler, Combust. Sci. Technol. **9**, 87 (1974) [Sov. J. Chem. Phys. (1984)].
[89]G. Yu. Grigor'ev, S. B. Dorofeev, and B. M. Smirnov, Khim. Fiz. **3**, 603 (1984) [Sov. J. Chem. Phys. (1984)].
[90]G. Yu. Grigor'ev, S. B. Dorofeev, B. N. Kuvshinov, and B. M. Smirnov, Fiz. Goreniya Vzryva, No. 5, 3 (1984) [Combust. Explos. Shock Waves (USSR) (1984)].
[91]M. Kh. Karapet'yants and M. L. Karapet'yants, *Fundamental Thermodynamic Constants of Inorganic and Organic Materials* (In Russian) Khimiya, M., 1968.
[92]A. I. Efimov *et al.*, *Properties of Inorganic Compounds-a handbook* (In Russian) Khimiya, L., 1983.
[93]N. N. Semenov, *Chain Reactions* (In Russian), ONTI, L., 1934.
[94]D. A. Frank-Kamenetskiĭ, *Diffusion and Heat Transfer in Chemical Kinetics*, Plenum Press, N.Y., 1969 [Russ. original, Nauka, M., 1967].
[95]V. N. Kondrat'ev and E. E. Nikitin, *Gas-Phase Reactions, Kinetics and Mechanisms*, Springer-Verlag, Berlin, 1981 [Russ. original, Nauka, M., 1974].
[96]Ya. B. Zel'dovich and D. A. Frank-Kamenetskiĭ, Dokl. Adad. Nauk SSSR **19**, 693 (1938).
[97]B. M. Smirnov, Phys. Rep. **152**, 177 (1987).
[98]B. M. Smirnov, Usp. Fiz. Nauk **160**, No. 4, 1 [Sov. Phys. Usp. **33**, 261 (1990)].
[99]P. Lecompte *et al.*, Phys. Scr. **23**, 376 (1981).
[100]G. Poelz and R. Riethmuller, Nucl. Instrum. Methods **195**, 491 (1982).
[101]S. Henning and L. Svensson, Phys. Scr. **23**, 697 (1981).
[102]S. Henning *et al.*, Phys. Scr. **23**, 703 (1981).
[103]S. Henning, in *Aerogels* (J. Fricke, Ed.), Springer-Verlag, Berlin, Heidelberg, New York, 1986, p. 38.

Translated by Frederick R. West